future transportation

MDPI

Article

Capacity Analysis of Intersections When CAVs Are Crossing in a Collaborative and Lane-Free Order

Mahdi Amouzadi *, Mobolaji Olawumi Orisatoki and Arash M. Dizqah

Smart Vehicles Control Laboratory (SVeCLab), University of Sussex, Brighton BN1 9RH, UK
* Correspondence: m.amouzadi@sussex.ac.uk

Abstract: Connected and autonomous vehicles (CAVs) improve the throughput of intersections by crossing in a lane-free order as compared to a signalised crossing. However, it is challenging to quantify such an improvement because the available frameworks to analyse the capacity of the conventional intersections do not apply to the lane-free ones. This paper proposes a novel framework including a measure and an algorithm to calculate the capacity of the lane-free intersections. The results show that a lane-free crossing of CAVs increases the capacity of intersections by 127% and 36% as compared to a signalised crossing of, respectively, human-driven vehicles and CAVs. The paper also provides a sensitivity analysis indicating that, in contrast to the signalised ones, the capacity of the lane-free intersections improves by an increase in the initial speed, maximum permissible speed and acceleration of vehicles.

Keywords: intersection throughput; traffic management; connected and autonomous vehicles; signal-free intersections; signalised intersection

check for updates

Citation: Amouzadi, M.; Orisatoki, M.O.; Dizqah, A.M. Capacity Analysis of Intersections When CAVs Are Crossing in a Collaborative and Lane-Free Order. *Future Transp.* **2022**, 2, 698–710. https://doi.org/10.3390/futuretransp2030039

Academic Editor : Jian Li

Received: 29 April 2022
Accepted: 22 July 2022
Published: 4 August 2022

Publisher's Note: MDPI stays neutral with regard to jurisdictional claims in published maps and institutional affiliations.

Copyright: © 2022 by the authors. Licensee MDPI, Basel, Switzerland. This article is an open access article distributed under the terms and conditions of the Creative Commons Attribution (CC BY) license (https://creativecommons.org/licenses/by/4.0/).

1. Introduction

Capacity analysis of intersections is essential for the planning and traffic management of transport systems. Unlike traditional human-driven vehicles (HVs), which are restricted to travel within the road lanes, connected and autonomous vehicles (CAVs) are capable of crossing through intersections in a lane-free order. There are extensive prior works to characterise the capacity of intersections for HVs (e.g., [1–3]); however, such analysis for CAVs in a lane-free order is still an open research topic.

The measures of capacity for HVs crossing both signalised and unsignalised (two-way stop-controlled and all-way stop-controlled) intersections are extensively discussed in Highway Capacity Manual (HCM) [1]. The manual introduces a measure to quantify the capacity of the unsignalised two-way and all-way stop-controlled intersections based on, respectively, gap acceptance and queuing theories. Meanwhile, it is recommended in [1] to calculate the capacity of the signalised intersections as the saturation flow rate times the green time ratio. All of these measures assume that headway of each HV in the queue of lanes is known to be around 1.9 s. This assumption makes these measures inappropriate for lane-free intersections where the headway of CAVs is much smaller and almost the same for all the vehicles in the queue [4].

Whilst human reaction is the dominant factor to measure capacity of intersections with HVs, CAVs are driverless vehicles with a shorter reaction time, which is not a dominant factor for their lane-free crossing. In addition, CAVs collaborate to keep a shorter safety distance than HVs. However, all these capabilities depend on the controller design of CAVs, which affect the indicative measure of the headway. In this light, previous studies employed a wide range of headway values for CAVs. For instance, the authors in [5,6], designed their CAV controllers based on a fixed headway of 0.9 s. Other studies [7–9] employed a stochastic headway with a value from 0.5 s up to 2 s based on four modes, namely aggressive, neutral, conservative, and safe. Therefore, it can be observed that capacity measurement of CAVs when passing through intersections can be different for each controller design and the chosen headway value.

To evaluate capacity of the intersections with CAVs, the authors in [4,10,11] employed the same measure that is defined in [1] for the unsignalised intersections, though with a new headway definition for CAVs. In [10], intersections are assumed as service providers and CAV headway is redefined as service time (i.e., crossing time), which is derived by applying queuing theory. The service time is based on the safety time gap of CAVs approaching the intersection from the same stream and from the conflicting streams. A similar work is proposed in [4] that employs the M/G/1 queue model to drive a formula for the capacity of the intersections. This model assumes that the intersection capacity is equivalent to the service rate of vehicles. Finally, the authors in [11] reformulated the capacity measure of the unsignalised two-way stop-controlled intersections to use the critical gap and follow-up time of CAVs instead of the ones of HVs. The measures provided by these researchers are effective to evaluate capacity of the intersections when CAVs drive through a restricted set of lanes; however, they are not applicable to the lane-free intersections. Hence, there is a need for a measure to quantify the capacity for the lane-free crossing of CAVs through intersections.

As it is previously mentioned, CAVs are heterogenous in terms of their control strategy [10] and any measure to quantify capacity of intersections must be independent of the performance of these strategies. However, the majority of the above-mentioned research measures the capacity of intersections with headway values which are dependent on the control strategy of CAVs which are particularly assumed to follow a reservation-based strategy.

The first type of reservation strategies is called intersection–reservation where the controller reserves the whole intersection for one CAV at a time. The authors in [12] formulated an optimal control problem (OCP) to minimise the crossing time of CAVs while reserving the whole intersection to avoid collisions. The references [13,14] introduce an intersection crossing algorithm where CAVs are placed into a virtual platoon based on their distance to the centre of the intersection. The algorithm reserves the whole intersection for each CAV in the platoon to pass through without collision. Generally speaking, reservation of the whole intersection reduces the capacity of the intersection.

The second type is a conflict–point–reservation strategy that reduces the area of reservation to just a few conflicting points. The authors in [15,16] designed optimisation-based algorithms to realise this type of reservation algorithms. A similar work is proposed in [17], where a constraint is added to the optimisation problem for each conflict point to limit the maximum number of crossing vehicles at any time to one. Even though the reservation-based strategies improve the capacity of intersections by nullifying the stop-and-go requirement of the conventional signalised intersections, yet vehicles must follow a set of predefined paths and are not able to fully utilise the intersection area by lane-free manoeuvres.

Alternatively, the authors in [18] developed an OCP to formulate the lane-free crossing problem of intersections. The objective of the developed OCP is to minimise the crossing time of CAVs and therefore the algorithm generates time-optimal trajectories for each CAV. However, the proposed OCP contains a set of highly non-convex constraints to represent the collision avoidance criteria which makes it difficult to solve online. To resolve this issue, Li et al. [18] splits the non-convex formulation into two stages. At stage one, which is solved online, CAVs make a standard multi-lane formation by moving to pre-defined positions of each lane. At stage two, the controller determines the crossing scenario based on destinations of CAVs in the formation (depending on number of lanes, the number of possible scenarios could be significantly high). The controller, then, fetches the optimal solution of the lane-free crossing of the CAVs of this particular scenario from a look-up table and enforces the CAVs to follow the pre-defined trajectories. The solution of the non-convex OCP for each scenario is already calculated offline and stored in the look-up table. The approach is scientifically interesting, but it is not practical because, for example, it takes around 356 years to solve the non-convex OCPs for all possible scenarios using the state-of-the-art processors when there are 24 CAVs [18].

In a more recent study, Li et al [19] changed the minimum-time OCP of [18] to a feasibility problem to make the non-convex formulation tractable. However, this results in a sub-optimal solution. The authors in [20] resolved the previous issues by using dual problem theory to convexify the non-convex constraints that avoid CAVs colliding with each other and with road boundaries. This work generates time-optimal trajectories of CAVs passing through intersections in a lane-free order and shows that such a lane-free crossing reduces the travelling time by up to 65% as compared to the state-of-the-art reservation-based method proposed in [21].

Figure 1 summarises different measures that are proposed by prior works to calculate the capacity of intersections for both HVs and CAVs.

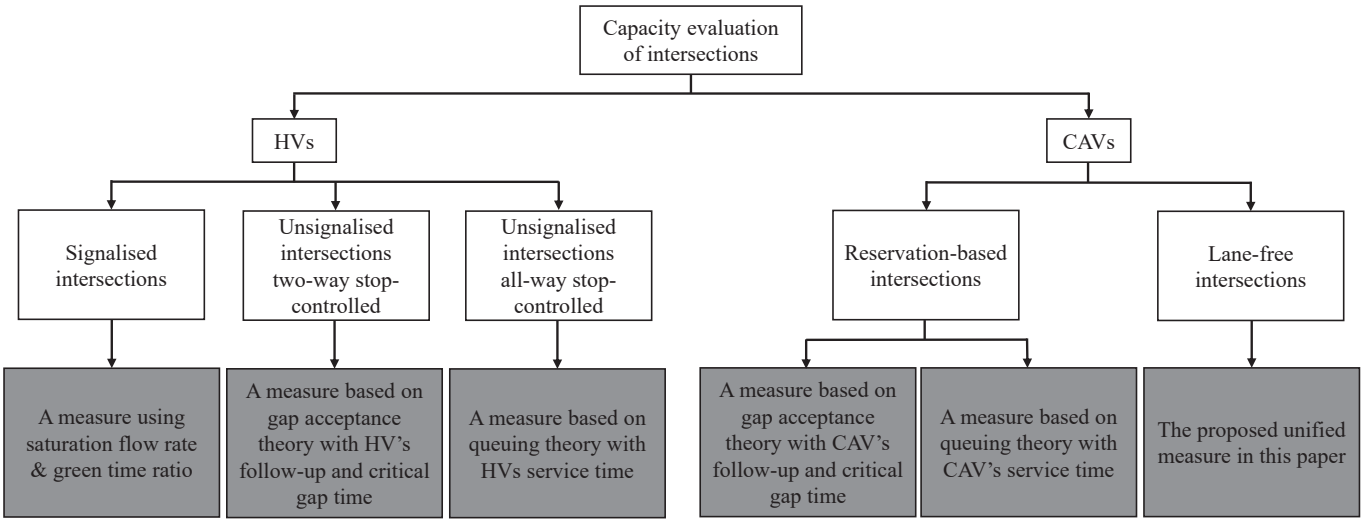


Figure 1. The measures for capacity evaluation of intersections (grey boxes) with both the human-driven vehicles (HVs) and connected and autonomous vehicles (CAVs).

This paper addresses the above-mentioned gap, i.e., the lack of a measure to quantify the capacity of lane-free intersections regardless of control strategies, by the following contributions to the knowledge:

- A novel framework to evaluate the capacity of lane-free intersections regardless of the crossing scenario. The framework consists of a novel measure of capacity along with an algorithm to calculate this measure.
- Assessment of the efficacy of lane-free crossing to the capacity of intersections as compared to the signalised crossing of HVs and CAVs.
- A sensitivity analysis of the capacity and crossing time of the lane-free intersections with respect to the maximum speed, maximum acceleration/deceleration, initial speed, and the number of the crossing vehicles.

The remainder of this paper is structured as follows: Section 2 provides the theoretical scheme that represents the lane-free intersections in this study. Section 3 introduces the proposed framework including a novel measure and a calculating algorithm for the capacity of the lane-free intersections. The capacity improvement of lane-free intersections as compared to signalised intersections is demonstrated in Section 4. A sensitivity analysis of the calculated capacity with respect to the variation of the speed and acceleration of the crossing vehicles is provided in Section 5, which is followed by a conclusion in Section 6.

2. System Description

Figure 2 shows an example of the lane-free and signal-free intersections. The example is composed of four approaches, each with three incoming and three outgoing lanes. The colour brightness of the crossing CAVs changes from solid at the starting point to the most transparent at the destination. Lane-free intersections allow CAVs to change their lanes at

any point of journey that helps to travel faster. For instance, the red CAV in Figure 2 takes over the black CAV by travelling through the opposite lane. Moreover, this intersection has no traffic light and CAVs collaborate to cross safely and quickly. An example of the lane-free crossing of intersections is provided as a video https://youtu.be/6RaNmro5D1k (accessed on 1 August 2022).. This study focuses on the globally optimum crossing of CAVs and assumes that there is a centralised controller for this purpose.

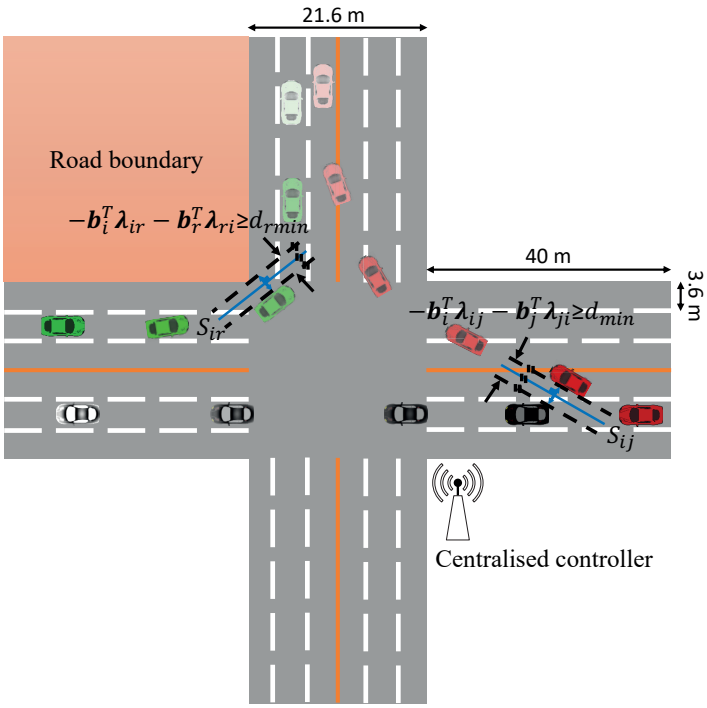


Figure 2. Layout of the studied lane-free and signal-free intersection which also shows the sufficient conditions for obstacle avoidance. Further details are presented in Section 3.2.

Figure 2 also illustrates the sufficient conditions of $-\boldsymbol{b_i}^\top\boldsymbol{\lambda}_{ij} - \boldsymbol{b_j}^\top\boldsymbol{\lambda}_{ji} \geq d_{min}$ and $-\boldsymbol{b_i}^\top\boldsymbol{\lambda}_{ir} - \boldsymbol{b_r}^\top\boldsymbol{\lambda}_{ri} \geq d_{rmin}$ to, respectively, avoid collisions between the red and black CAVs and between the green CAV and road boundary. These conditions are extracted after applying the dual problem theory to the minimum distance problem between two polytopes. d_{min} and d_{rmin} are, respectively, the minimum permissible distances between the vehicles and between the vehicles and road boundaries. $\mathbf{b}_{i/j/r}$ are related to the size of polytopes representing $\text{CAV}_{i/j}$ and road boundaries and $\boldsymbol{\lambda}_{ij}$, $\boldsymbol{\lambda}_{ji}$ and $\mathbf{s}_{ij}$ are dual variables. More details are presented in Section 3.2 and for further details; the reader is referred to [20].

3. A Novel Framework to Quantify Capacity of the Lane-Free Intersections

Conventionally, the capacity of intersections (both the signalised and unsignalised) is measured using a set of collected data from either real-time observation of vehicles [1] or running a micro-simulation [22,23]. For example, capacity of each lane of an unsignalised all-way stop-controlled (AWSC) intersection is measured by gradually increasing the flow rate of the lane in the simulator until the degree of utilisation (DoU) of the lane reaches one, which happens when throughput of the lane is equal to its capacity.

DoU represents the fraction of capacity being used by vehicles and is defined as follows [1]:

$$x = \frac{vh_d(x)}{3600} \tag{1}$$

where x denotes the degree of utilisation, v refers to flow rate (throughput) (veh/h) of the lane and h_d is the departure headway (s) that is a function of x and is calculated as a stochastically weighted average of the saturation headway of all combinations of possible degrees of conflict and the number of crossing vehicles. The reference [1] proposes an iterative algorithm to calculate the value of x and h_d for any given v based on the identified values from the available large set of real data.

However, such real-time data are not available for lane-free crossing of CAVs because of the lack of real infrastructure or realistic simulators that consider the collaborative behaviour of enough number of heterogeneous CAVs crossing an intersection. The remainder of this section introduces a new measure and a calculating algorithm of the capacity of lane-free intersections.

3.1. The Proposed Measure of the Capacity

Intersections can host a limited number of vehicles at the same time and, if the intersection capacity exceeds the waiting time of crossing vehicles will significantly increase. Therefore, to evaluate the capacity of intersections, a suitable measure must consider the maximum number of vehicles and the time that it takes for those vehicles to pass through the intersection. In effect, the following measure is proposed to calculate the capacity of the lane-free intersections:

$$C = max\{\frac{3600 \times N}{T}\} \tag{2}$$

where C is the capacity (veh/h) of the intersection, N denotes the number of crossing CAVs (veh) and T represents the time (s) that takes for those vehicles to fully cross the intersection.

Equation (2) requires a simulator to gradually increase the number of vehicles N and measuring their minimum crossing time T_{min} to calculate the throughput $3600 \times N/T_{min}$ until the throughput starts dropping. The last value of the throughput just before dropping is the capacity of the intersection.

The next sections present methods to find N and T for the lane-free and signalised intersections.

3.2. The Proposed Algorithm to Calculate the Capacity

The central theme of the proposed algorithm to solve (2) is to use the minimum-time crossing method in [20] to calculate the minimum crossing time T_{min} of the lane-free intersections for a given number N of CAVs. It is already shown in [20] that, unlike the signalised intersections, the crossing time of CAVs in a lane-free order is independent of the scenario (i.e., the initial positions and destinations of vehicles). Thus, Equation (2) is solved for a sample scenario with a low number of crossing CAVs (e.g., three) and then new CAVs are gradually added to the scenario until the throughput reaches the capacity as explained above. This method can also be applied to calculate the maximum throughput of the signalised intersections for a given scenario. This sub-section provides a summary of the method and, for further details, the reader is referred to [20].

In this study, a CAV_i is represented with a two degree-of-freedom (DoF) bicycle model [24] of its lateral motion. The chosen variables as DOFs are the sideslip angle β_i and the yaw rate r_i. The longitudinal motion of the vehicle, on the other hand, is modelled by the longitudinal speed V_i of the vehicle as the only DoF. The following differential equations present the vehicle model of CAV_i, where $i \in \{1 \dots N\}$ and N is the total number of CAVs:

$$\frac{d}{dt}\begin{bmatrix} r_i \\ \beta_i \\ V_i \\ x_i \\ y_i \\ \theta_i \end{bmatrix}(t) = \begin{bmatrix} \frac{N_r}{I_z} \cdot r_i(t) + \frac{N_\beta}{I_z} \cdot \beta_i(t) \\ (\frac{Y_r}{m \cdot V_i(t)} - 1) \cdot r_i(t) + \frac{Y_\beta}{m \cdot V_i(t)} \cdot \beta_i(t) \\ 0 \\ V_i(t) \cdot cos\theta_i(t) \\ V_i(t) \cdot sin\theta_i(t) \\ r_i(t) \end{bmatrix} + \begin{bmatrix} 0 & \frac{N_\delta}{I_z} \\ 0 & \frac{Y_\delta}{m \cdot V_i(t)} \\ 1 & 0 \\ 0 & 0 \\ 0 & 0 \\ 0 & 0 \end{bmatrix} \begin{bmatrix} a_i \\ \delta_i \end{bmatrix}(t) \tag{3}$$

where the control inputs and states of CAV$_i$ are presented as $\boldsymbol{u} = [a_i, \delta_i]^T$ and $\boldsymbol{x} = [r_i, \beta_i, V_i, x_i, y_i, \theta_i]^T$, respectively. The pose of CAV$_i$ at time t is denoted as $\boldsymbol{z}_i(t) = [x_i(t), y_i(t), \theta_i(t)]^T$. $\delta_i(t)$ and $a_i(t)$ are the wheel steering angle (rad) and acceleration (m/s^2) of CAV$_i$. The constants m and I_z represent, respectively, the mass (kg) of the vehicle and its moment of inertia (kg·m^2) around axis z. The vehicle parameters Y_r, Y_β, Y_δ, N_r, N_β and N_δ are calculated as in [24].

To ensure CAVs drive within their admissible range, the following constraints are imposed for each CAV$_i$:

$$\underline{V} \leq V_i(t) \leq \bar{V}, \tag{4}$$
$$\underline{a} \leq a_i(t) \leq \bar{a}, \tag{5}$$
$$\underline{\delta} \leq \delta_i(t) \leq \bar{\delta}, \tag{6}$$
$$\underline{r} \leq r_i(t) \leq \bar{r}, \tag{7}$$
$$\underline{\beta} \leq \beta_i(t) \leq \bar{\beta}. \tag{8}$$

where $\underline{.}$ and $\bar{.}$ are the lower and upper boundaries, respectively.

To formulate the obstacle avoidance constraints, each CAV$_i$ is presented as a rectangular polytope ζ_i representing the area within the intersection of the linear inequality $\mathbf{A}_i\mathbf{x} \leq \mathbf{b}_i$, where $\mathbf{x} = [x, y]^T$ is a Cartesian point. CAV$_i$ and CAV$_j$ $\forall i \neq j \in \{1 \dots N\}$ collide if their polytopic sets intersect, i.e., $\zeta_i \cap \zeta_j \neq \emptyset$. This is a non-convex and non-differentiable constraint and is replaced by the following sufficient condition [20]:

$$dist(\zeta_i, \zeta_j) = \min_{\mathbf{x},\mathbf{y}} \{\|\mathbf{x} - \mathbf{y}\|_2 \mid \mathbf{A}_i\mathbf{x} \leq \mathbf{b}_i,\ \mathbf{A}_j\mathbf{y} \leq \mathbf{b}_j\} \geq d_{min}; \quad \forall i \neq j \in \{1..N\}. \tag{9}$$

where d_{min} is a minimum safety distance between any pair of CAVs.

Road boundaries are also modelled with convex polytopic sets $\mathcal{O}_r$ where $r \in \{1 \dots N_r\}$, and N_r denotes the total number of road boundaries, which is 4 for a four-legged intersection. A similar sufficient condition to (9) is defined for each pair of CAV$_i$ and boundary r to avoid collision (i.e., $\zeta_i \cap \mathcal{O}_r \neq \emptyset$).

The lane-free crossing problem is defined as an OCP that minimises the crossing time while avoiding collisions (see [20]):

$$\{a_i(.), \delta_i(.)\}^* = \tag{10}$$
$$\arg\underset{\substack{t_f, a_i(.), \delta_i(.) \\ \boldsymbol{\lambda}_{ij}, \boldsymbol{\lambda}_{ji}, \mathbf{s}_{ij}, \\ \boldsymbol{\lambda}_{ri}, \lambda_{ir}, \mathbf{s}_{ir}}}{\text{minimise}} J(\mathbf{z}_1(.), .., \mathbf{z}_N(.))$$
$$\text{s.t.} \quad \text{Equations (3)–(8)} \tag{11}$$
$$-\mathbf{b}_i(\mathbf{z}_i(t))^\top \boldsymbol{\lambda}_{ij}(t) - \mathbf{b}_j(\mathbf{z}_j(t))^\top \boldsymbol{\lambda}_{ji}(t) \geq d_{min} \tag{12}$$
$$\mathbf{A}_i(\mathbf{z}_i(t))^\top \boldsymbol{\lambda}_{ij}(t) + \mathbf{s}_{ij}(t) = 0 \tag{13}$$
$$\mathbf{A}_j(\mathbf{z}_j(t))^\top \boldsymbol{\lambda}_{ji}(t) - \mathbf{s}_{ij}(t) = 0 \tag{14}$$
$$-\mathbf{b}_i(\mathbf{z}_i(t))^\top \boldsymbol{\lambda}_{ir}(t) - \mathbf{b}_r^\top \boldsymbol{\lambda}_{ri}(t) \geq d_{rmin} \tag{15}$$
$$\mathbf{A}_i(\mathbf{z}_i(t))^\top \boldsymbol{\lambda}_{ir}(t) + \mathbf{s}_{ir}(t) = 0 \tag{16}$$
$$\mathbf{A}_r^\top \boldsymbol{\lambda}_{ri}(t) + \mathbf{s}_{ir}(t) = 0 \tag{17}$$
$$\boldsymbol{\lambda}_{ij}(t),\ \boldsymbol{\lambda}_{ji}(t),\ \boldsymbol{\lambda}_{ir}(t),\ \boldsymbol{\lambda}_{ri}(t) \geq 0, \tag{18}$$
$$\left\|\mathbf{s}_{ij}(t)\right\|_2 \leq 1,\ \left\|\mathbf{s}_{ir}(t)\right\|_2 \leq 1, \tag{19}$$
$$\mathbf{z}_i(t_0) = \mathbf{z}_{i,0},\ \mathbf{z}_i(t_f) = \mathbf{z}_{i,f}, \tag{20}$$
$$\forall i \neq j \in \{1..N\}, \forall r \in \{1..N_r\}.$$

where i, j and r refer to, respectively, CAV_i, CAV_j and rth road boundary. $\mathbf{A}_i$ and $\mathbf{b}_i$ represent the size and orientation of CAV_i which are functions of the CAV_i's pose $\mathbf{z}_i(t)$. Equations (12)–(17) constrain CAVs to avoid collisions and are derived from (9) using the dual problem theory, where $\boldsymbol{\lambda}_{ij}, \boldsymbol{\lambda}_{ji}, \mathbf{s}_{ij}, \boldsymbol{\lambda}_{ri}, \boldsymbol{\lambda}_{ir}, \mathbf{s}_{ir}$ are dual variables [20]. Details are provided in [25]. As a summary, Figure 2 shows that $\mathbf{s}_{ij}$ and $\mathbf{s}_{ir}$ are the separating hyperplanes and $-\mathbf{b}_i^\top \boldsymbol{\lambda}_{ij} - \mathbf{b}_j^\top \boldsymbol{\lambda}_{ji}$ and $-\mathbf{b}_i^\top \boldsymbol{\lambda}_{ir} - \mathbf{b}_r^\top \boldsymbol{\lambda}_{ri}$ represent distances between, respectively, two CAVs and a CAV and road boundary.

Problem (10) is nonlinear and is solved using CasADi [26] and IPOPT [27] for any given number N of CAVs and their initial locations to find the minimum crossing time t_f. The solution consists of the final time t_f and the optimal trajectories of control inputs $a_i(.)^*$ and $\delta_i(.)^*$ for each CAV_i over $t \in [t_0, t_f]$. Details on the computational time of (10) are provided in [20]. However, the computational time does not affect the proposed capacity analysis because it is performed offline.

4. Capacity Analysis of the Lane-Free Intersections

The capacity of the lane-free intersection in Figure 2 is calculated in this section based on the measure (2) and using the introduced algorithm in Section 3.2 that computes the minimum crossing time of CAVs for a given number of vehicles. Table 1 summarises the critical parameters that are used throughout the calculations.

Table 1. Main parameters of the proposed algorithms and their values.

Parameter(s)	Unit	Value(s)
Maximum speed	(m/s)	25
Maximum acceleration	(m/s^2)	3
Initial speed	(m/s)	10
Prediction horizon	($\times$ sampling times)	15
Safe margin between CAVs	(m)	0.1
Vehicle length	(m)	4.5
Vehicle width	(m)	1.8

Figure 3a shows the calculated minimum crossing times which are fairly constant for a wide range of the number of crossing CAVs. However, there is a sharp increase after exceeding the threshold of 15 crossing CAVs showing that the capacity is reached. Equation (2) is used to measure throughput of the intersection based on the calculated minimum crossing times and the peak of the calculated throughput is the capacity of the intersection. Figure 3b illustrates that the capacity of the studied lane-free intersection is 10,800 $CAVs/h$ where the throughput starts dropping.

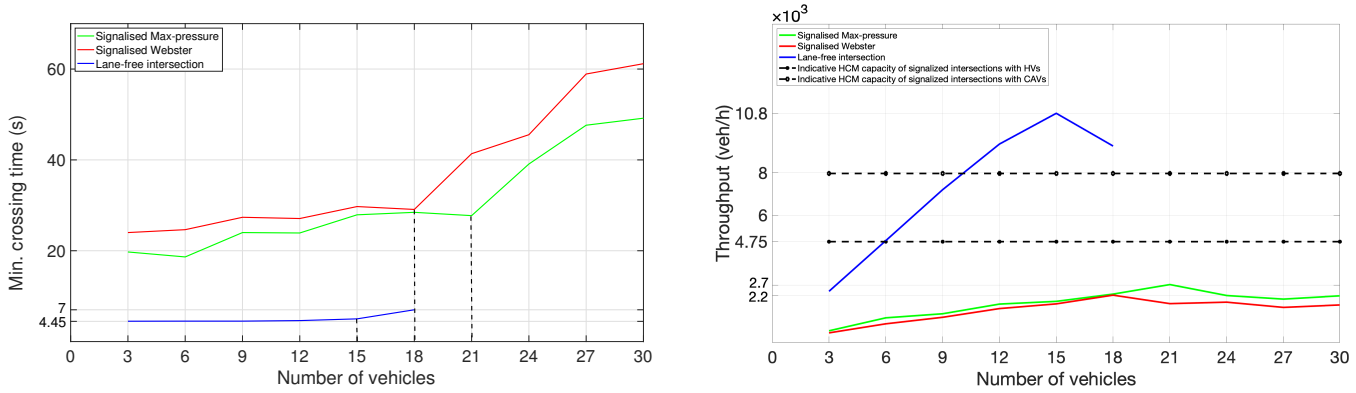


Figure 3. (**a**) The calculated crossing times by the lane-free algorithm and signalised max-pressure and Webster controllers for different number of vehicles; (**b**) the corresponding throughput obtained by the proposed measure as well as HCM indicative capacity of signalised intersections for both HVs and CAVs. The headway of CAVs is assumed as 1.13 s, which is an average of the provided stochastic values in [28].

To compare the capacity of the lane-free intersection against signalised intersections, this study employs the HCM [1] capacity calculations for the signalised intersection with HVs. HCM defines the capacity of signalised intersections based on the saturation flow rate of each lane multiplied by a green ratio f accounting for lost times due to changing phases. Considering a cycle length of 120 s and a lost time of 5 s, the green ratio is $f = \frac{120-4\times5}{120} = 0.8\bar{3}$. Thus, a recommended saturation flow rate of 1900 HVs/h/ln gives the capacity of the three-lane intersection in Figure 2 as $1900 \times 3 \times 0.8\bar{3} = 4750$ HVs/h, which is called hereby as the HCM indicative capacity of the signalised intersection with HVs. Figure 3b displays the calculated value of this indicative capacity as a horizontal line. It is worth noting that the HCM indicative capacity is independent of the number of crossing vehicles and is overlapped just for comparison. Figure 3b shows that the capacity of the studied intersection when CAV crossing in a lane-free order is 127% higher than the capacity of the same intersection when signalised and with HVs. This massive jump in capacity is due to the fact that CAVs have shorter headway, do not stop by traffic lights and, most importantly, collaborate to utilise the maximum spatial-temporal area of the intersection to minimise the crossing time.

In case of only CAVs crossing the signalised intersection, the capacity increases due to a shorter headway of CAVs compared to HVs. However, there is not an exact value for the headway of CAVs because this value significantly depends on the controller behaviour and hence path planning algorithms of CAVs. In this light, there is wide range of headway values provided in the literature [28–30]. The present work considers a headway of 1.13 s for CAVs which is an average of the provided stochastic values in [28]. Thus, the saturation flow rate of each lane is increased to 3186 CAVs/h and the capacity of the same signalised intersection for CAVs is calculated as 7964 CAVs/h. This indicative HCM capacity of signalised intersections with CAVs is shown in Figure 3b to compare with the lane-free intersection. As it can be seen, the strategy of lane-free crossing improves the capacity of the intersection by 36% as compared to signalised crossing with CAVs.

However, using the concept of the saturated flow rate to calculate the capacity of a signalised intersections with crossing CAVs seems not to be accurate because: (i) there is a large discrepancy in the reported values of the CAVs' headway, (ii) the previously reported headway of CAVs did not consider the collaborative and heterogeneous nature of the algorithms of CAVs, and (iii) lateral dynamics of the vehicles on the truing lanes are not considered for the calculation of the saturation flow rate. In fact, the provided results in this paper for the capacity of the lane-free intersection suggest that an indicative value for the CAVs' headway $T_{h,CAVs}$ can not be smaller than 0.83 s ($T_{h,CAVs} \geq \frac{3\times3600\times0.83}{10800} \geq 0.83$).

As previously mentioned, unlike the capacity of lane-free intersections, the capacity of signalised ones depends on the crossing scenario. To show this, two adaptive traffic controllers, max-pressure [31] and Webster [32], are applied to the same intersection for the same scenario as the lane-free intersection. Both the max-pressure and Webster algorithms are simulated in SUMO with the help of TraCI for gradually increasing number of HVs based on the works in [33]. Webster in [32] derived a formulation that calculates the cycle length of traffic lights. The derived cycle length is used to find the green time of each phase to allow vehicles to cross the intersection. Similarly, the max-pressure algorithm computes the signal timings; however, the green time of each phase is calculated based on the number of vehicles in the incoming and outgoing lanes [31]. Whilst Webster is a well-known algorithm for timing control of traffic lights, it is already shown that the max-pressure algorithm yields the lowest travelling time, queues length and crossing delays among all the state-of-the-art controllers [33], including the algorithms based on the self organising [34,35], deep Q-network [36], deep deterministic policy gradient [37] and Webster methods.

Figure 3 shows the SUMO simulated crossing times of a different number of HVs through a signalised version of the intersection in Figure 2 when the traffic lights are controlled by the max-pressure and Webster algorithms. As observed, the crossing time of max-pressure and Webster controllers increases significantly after the number of crossing vehicles exceeds the thresholds of, respectively, 21 and 18 vehicles. To calculate the corresponding maximum throughput for these adaptive controllers the measure (2) is employed and the results are shown in Figure 3b as compared to the lane-free intersection for the same crossing scenario. From Figure 3b, it can be seen that the maximum throughput of the scenario using two state-of-the-art traffic controllers are, respectively, 2726 (veh/h) and 2227 (veh/h). Hence, the capacity of the lane-free intersection is, respectively, 296% and 385% larger than the maximum throughput of max-pressure and Webster for that particular scenario. It is clear that the calculated maximum throughput values are not the same as HCM capacity of signalised intersections with HVs, and this indicates that the capacity of signalised intersections is dependent on the type of scenario. This difference is due to HCM capacity calculations assuming that an unlimited number of vehicles are queued in lanes; however, this might not be true in the real world. Therefore, the proposed measure (2) and the SUMO simulator of max-pressure and Webster controllers can be employed to calculate the maximum throughput of signalised intersections for any desired scenario.

5. Sensitivity Analysis of the Capacity and Crossing Time of the Lane-Free Intersections

Figure 4a,b, respectively, show the variation of the crossing time and the normalised capacity of the studied lane-free intersection due to changes in the maximum speed and acceleration of CAVs. As seen, the larger the maximum permissible speed and acceleration of the vehicles are, the shorter the crossing time and equivalently the larger the capacity that are achieved. The capacity of the intersection reaches to its top value when the maximum allowed speed and acceleration are, respectively, 30 (m/s) and 4 (m/s^2). The initial speed of vehicles is 10 (m/s). Apparently, and as shown in Figure 4, relaxing the range of acceleration without expanding the range of speed has a very limited effect on the capacity.

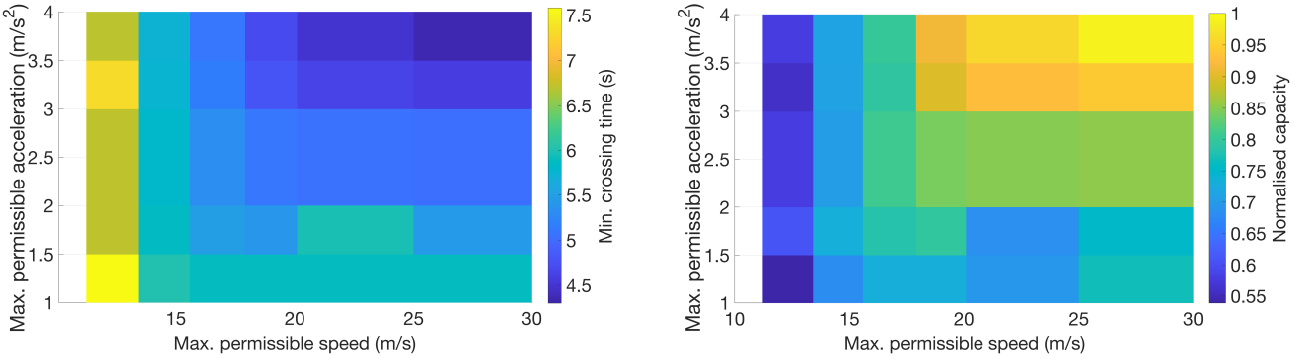


Figure 4. Sensitivity of the (**a**) crossing time and (**b**) capacity of the lane-free intersection in terms of the maximum speed and acceleration of CAVs. Initial speed of the vehicles is 10 (m/s).

Figure 5 provides more details on the results of Figure 4. Samples of the results in Figure 4 for two different values of the maximum permissible accelerations and speeds are illustrated separately in Figure 5. As seen, the best crossing time of CAVs and equivalently the maximum capacity of the lane-free intersection improves by 28% due to an increase of the maximum acceleration from 2 (m/s^2) to 4 (m/s^2), and when CAVs enter the control area of the intersection with the initial speed of 5 (m/s). Figure 5 also shows that, doubling the initial speed from 5 (m/s) to 10 (m/s), the best crossing time and hence the maximum capacity increase by, respectively, 28% and 19% for the maximum accelerations of 2 (m/s^2) and 4 (m/s^2).

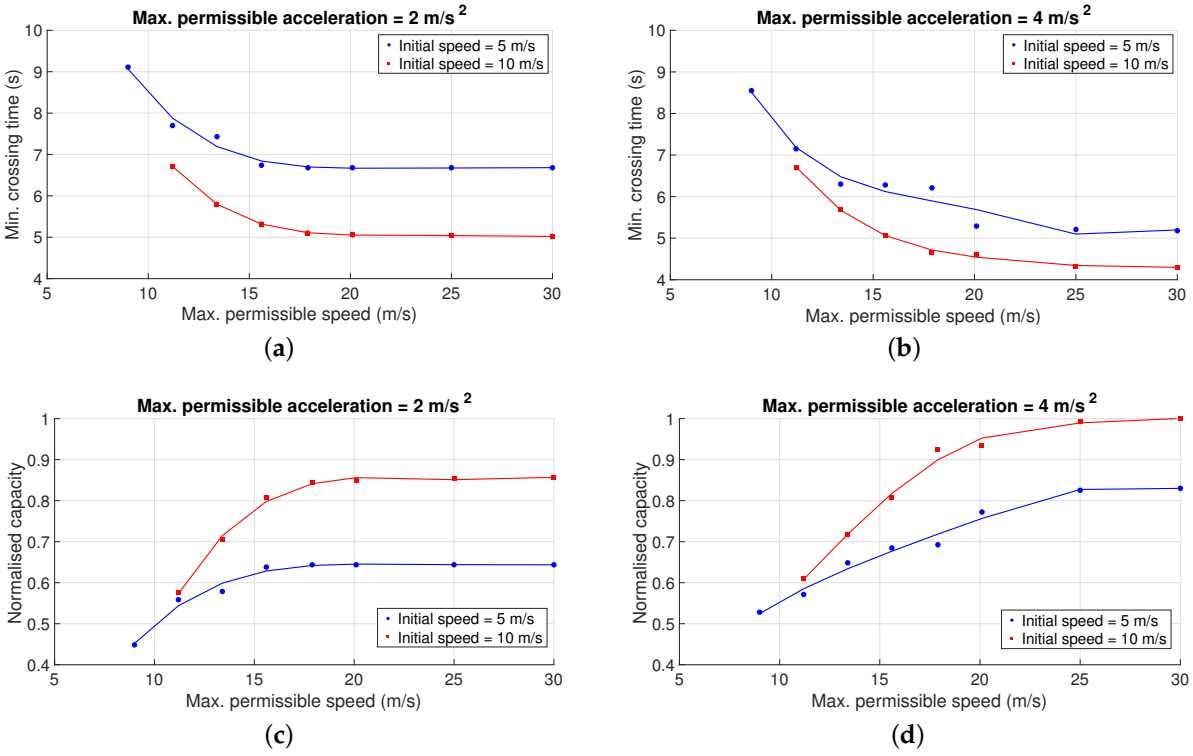


Figure 5. Variations of the crossing time when (**a**) Max. permissible acceleration is 2 m/s^2 and (**b**) Max. permissible acceleration is 4 m/s^2 and variations of capacity when (**c**) Max. permissible acceleration is 2 m/s^2 and (**d**) Max. permissible acceleration is 4 m/s^2 of the studied lane-free intersection over different values of the initial speed and the maximum permissible speed of CAVs. The solid lines are the corresponding fitted polynomials of order four, which show the variation trends.

Furthermore, Figure 5 shows that the maximum permissible speed also affects the minimum crossing time of CAVs and hence the capacity of the lane-free intersections to a certain limit. As shown, the capacity of the studied lane-free intersection increases logarithmically with a factor of 44% by raising the limit of the maximum permissible speed of CAVs up to around 18 (m/s) when the maximum allowable acceleration is 2 (m/s^2) (and 54% when it is 25 (m/s) at the maximum allowable acceleration fo 4 (m/s^2)). The capacity stays steady after these limits.

Figure 6, on the other hand, provides a similar analysis of the minimum crossing time and equivalently maximum throughput of the intersection in Figure 2 when there is a traffic light that controls the flow of intersection with the max-pressure and Webster state-of-the-art algorithms. Unlike the results in Figure 5, Figure 6 shows that the maximum throughput of the same intersection, when it is signalised, it is only slightly sensitive to the maximum permissible acceleration and does not vary by increasing the maximum allowable or initial speeds of the crossing vehicles. This is because of the fact that traffic lights oblige HVs to stop before the signalised intersections no matter what the vehicles' speed are, whilst CAVs can cross the lane-free intersections at all directions continuously and with no interruptions. The crossing time T of these stopped vehicles is dominated by the human reaction time with a mean fixed to a constant value. Hence, referring to Equation (2), maximum throughput of the signalised intersections is insensitive to the parameters and is dominant by the human factors.

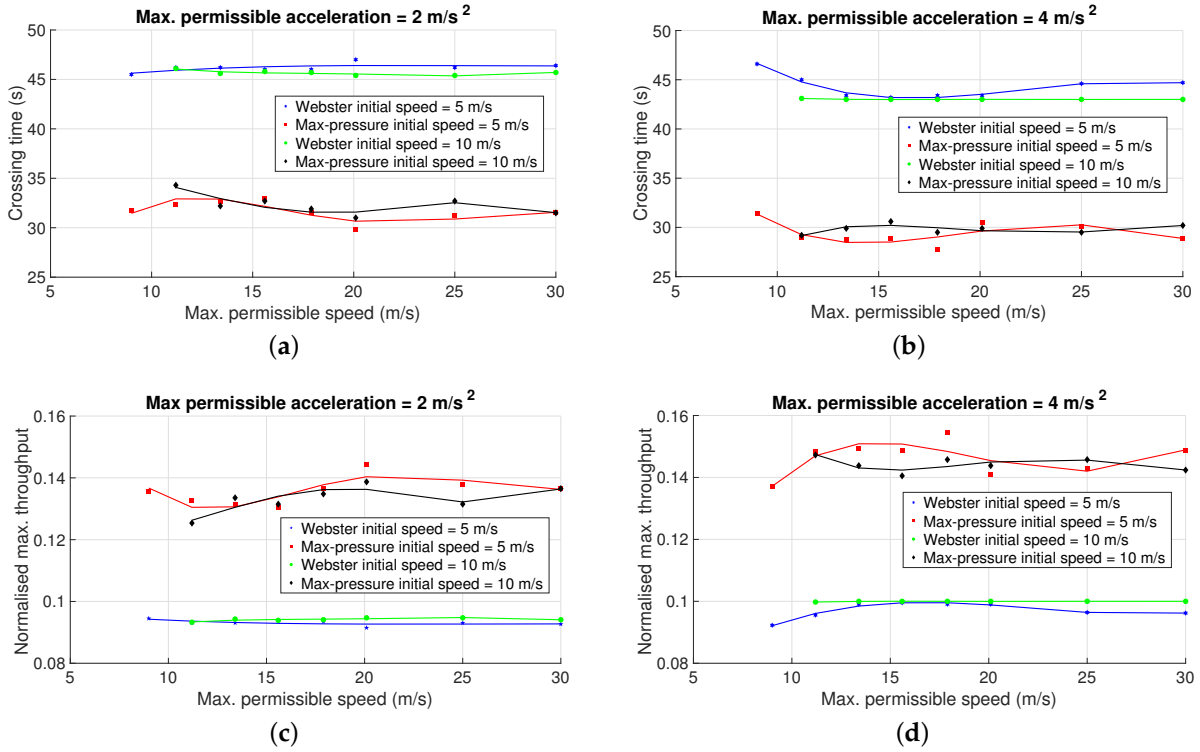


Figure 6. Variations of the crossing time when (**a**) Max. permissible acceleration is 2 m/s^2 and (**b**) Max. permissible acceleration is 4 m/s^2 and variations of maximum throughput when (**c**) Max. permissible acceleration is 2 m/s^2 and (**d**) Max. permissible acceleration is 4 m/s^2 of the signalised intersection for different values of the initial speed and the maximum permissible speed of the crossing HVs. The solid lines show trends of the variation as polynomials of order four.

6. Conclusions

Whilst it is known that the lane-free crossing of CAVs through intersections improves the capacity as compared to the signalised crossing of human drivers, to the best knowledge of the authors, there is no previous analysis that objectively quantifies such improvements. This is because: (i) the conventional capacity measures are not applicable to the lane-

free crossing, and (ii) the crossing performance of CAVs depends on the collaborative behaviour of the vehicles and not the performance of traffic light controller (as in conventional intersections) or individual vehicle (as in autonomous vehicles without such collaborative behaviour).

This work introduces a measure to represent the capacity of a given intersection when CAVs are crossing in a lane-free order, along with an algorithm to calculate the measure. The presented results show that the lane-free crossing of CAVs improves capacity of an intersection by, respectively, 127% and 36% as compared to capacity of the signalised crossing of human drivers and CAVs through the same intersection, which are calculated using highway capacity manual. A sensitivity analysis is also presented showing that, unlike the unresponsive maximum throughput of the signalised crossing to the variation of the initial speed and the maximum permissible crossing speed and acceleration of vehicles, an increase with either of these parameters improves the performance of the lane-free crossing to a degree.

This work also provides a benchmark to evaluate the performance of the algorithms to collaboratively cross CAVs through intersections. Future work will extend the provided analysis to the case with multiple intersections that consider more factors such as passenger comfort into the measurement of capacity.

Author Contributions: Conceptualization: M.A. and A.M.D.; data curation: M.A.; formal analysis: M.A. and A.M.D.; Methodology: M.A. and A.M.D.; validation: M.A. and A.M.D.; writing—original draft: M.A.; investigation: M.A.; visualisation: M.O.O.; writing—review and editing: M.O.O. and A.M.D.; software: A.M.D. and M.A.; supervision: A.M.D.; project administration: A.M.D. and M.A. All authors have read and agreed to the published version of the manuscript.

Funding: This research received no external funding.

Institutional Review Board Statement: Not applicable.

Informed Consent Statement: Not applicable.

Data Availability Statement: Not applicable.

Conflicts of Interest: The authors declare no conflict of interest.

References

1. Transportation Research Board; National Research Council. *Highway Capacity Manual*; Transportation Research Board; National Research Council: Washington, DC, USA, 2000.
2. Farivar, S. *Modeling Capacity and Delay at Signalized Intersections With Channelized Right-Turn Lanes Considering the Impact of Blockage*; Ph.D. Thesis, University of Nevada, Reno, NV, USA, 2015.
3. Wu, N.; Giuliani, S. Capacity and delay estimation at signalized intersections under unsaturated flow condition based on cycle overflow probability. *Transp. Res. Procedia* **2016**, *15*, 63–74. [CrossRef]
4. Wu, Y.; Zhu, F. Junction Management for Connected and Automated Vehicles: Intersection or Roundabout? *Sustainability* **2021**, *13*, 9482. [CrossRef]
5. Mohajerpoor, R.; Ramezani, M. Mixed flow of autonomous and human-driven vehicles: Analytical headway modeling and optimal lane management. *Transp. Res. Part Emerg. Technol.* **2019**, *109*, 194–210. [CrossRef]
6. Zhao, L.; Malikopoulos, A.A.; Rios-Torres, J. On the traffic impacts of optimally controlled connected and automated vehicles. In Proceedings of the Conference on Control Technology and Applications (CCTA), Hong Kong, China, 19–21 August 2019; pp. 882–887.
7. VanderWerf, J.; Shladover, S.; Kourjanskaia, N.; Miller, M.; Krishnan, H. Modeling effects of driver control assistance systems on traffic. *Transp. Res. Rec.* **2001**, *1748*, 167–174. [CrossRef]
8. Ivanchev, J.; Knoll, A.; Zehe, D.; Nair, S.; Eckhoff, D. Potentials and implications of dedicated highway lanes for autonomous vehicles. *arXiv* **2017** arXiv:1709.07658.
9. Altay, İ.; Aksun Güvenç, B.; Güvenç, L. Lidar data analysis for time to headway determination in the drivesafe project field tests. *Int. J. Veh. Technol.* **2013**, *2013*, 749896. [CrossRef]
10. Yu, C.; Sun, W.; Liu, H.X.; Yang, X. Managing connected and automated vehicles at isolated intersections: From reservation-to optimization-based methods. *Transp. Res. Part Methodol.* **2019**, *122*, 416–435. [CrossRef]
11. Li, L.; Gan, J.; Yang, F.; Ran, B.; Zhang, J. A method to calculate the capacity of unsignalized intersection for connected and automated vehicles based on gap acceptance theory. In Proceedings of the CICTP 2019, Nanjing, China, 6–8 July 2019; pp. 5600–5612.

12. Pan, X.; Chen, B.; Evangelou, S.A.; Timotheou, S. Optimal Motion Control for Connected and Automated Electric Vehicles at Signal-Free Intersections. In Proceedings of the 59th IEEE Conference on Decision and Control (CDC), Jeju Island, South Korea, 14–18 December 2020; pp. 2831–2836.
13. Xu, B.; Li, S.E.; Bian, Y.; Li, S.; Ban, X.J.; Wang, J.; Li, K. Distributed conflict-free cooperation for multiple connected vehicles at unsignalized intersections. *Transp. Res. Part Emerg. Technol.* **2018**, *93*, 322–334. [CrossRef]
14. Di Vaio, M.; Falcone, P.; Hult, R.; Petrillo, A.; Salvi, A.; Santini, S. Design and experimental validation of a distributed interaction protocol for connected autonomous vehicles at a road intersection. *IEEE Trans. Veh. Technol.* **2019**, *68*, 9451–9465. [CrossRef]
15. Wang, Y.; Cai, P.; Lu, G. Cooperative autonomous traffic organization method for connected automated vehicles in multi-intersection road networks. *Transp. Res. Part Emerg. Technol.* **2020**, *111*, 458–476. [CrossRef]
16. Mirheli, A.; Tajalli, M.; Hajibabai, L.; Hajbabaie, A. A consensus-based distributed trajectory control in a signal-free intersection. *Transp. Res. Part Emerg. Technol.* **2019**, *100*, 161–176. [CrossRef]
17. Zhang, H.; Zhang, R.; Chen, C.; Duan, D.; Cheng, X.; Yang, L. A Priority-Based Autonomous Intersection Management (AIM) Scheme for Connected Automated Vehicles (CAVs). *Vehicles* **2021**, *3*, 533–544. [CrossRef]
18. Li, B.; Zhang, Y.; Zhang, Y.; Jia, N.; Ge, Y. Near-optimal online motion planning of connected and automated vehicles at a signal-free and lane-free intersection. In Proceedings of the IEEE Intelligent Vehicles Symposium (IV), Suzhou, China, 26–30 June 2018; pp. 1432–1437.
19. Li, B.; Zhang, Y.; Jia, N.; Peng, X. Autonomous Intersection Management over Continuous Space: A Microscopic and Precise Solution via Computational Optimal Control. *IFAC-PapersOnLine* **2020**, *53*, 17071–17076. [CrossRef]
20. Amouzadi, M.; Orisatoki, M.O.; Dizqah, A.M. Lane-Free Crossing of CAVs through Intersections as a Minimum-Time Optimal Control Problem. In Proceedings of the 11th IFAC Symposium on Intelligent Autonomous Vehicles Prague, Czech Republic, 6–8 July 2022. [CrossRef]
21. Malikopoulos, A.A.; Beaver, L.; Chremos, I.V. Optimal time trajectory and coordination for connected and automated vehicles. *Automatica* **2021**, *125*, 109469. [CrossRef]
22. Chaudhry, M.S.; Ranjitkar, P. Capacity Analysis of Signalised Intersection Using Micro-Simulation. Ph.D. Thesis, University of Auckland, Auckland, New Zealand, 2009.
23. Chauhan Boski, P.; Joshi Gaurang, J.; Purnima, P. Microscopic Traffic Simulation Approach to Evaluate Driving Parameters at Influence Zone of the Intersection. In *Intelligent Infrastructure in Transportation and Management*; Springer: Singapore 2022; pp. 13–26.
24. Milliken, W.; Milliken, D. *Race Car Vehicle Dynamics*; Premiere Series; Society of Automotive Engineers Warrendale: Warrendale, PA, USA, 1995; Chapter 5.
25. Firoozi, R.; Ferranti, L.; Zhang, X.; Nejadnik, S.; Borrelli, F. A Distributed Multi-Robot Coordination Algorithm for Navigation in Tight Environments. *arXiv* **2020** arXiv:2006.11492.
26. Andersson, J.A.E.; Gillis, J.; Horn, G.; Rawlings, J.B.; Diehl, M. CasADi–A software framework for nonlinear optimization and optimal control. *Math. Program. Comput.* **2019**, *11*, 1–36. [CrossRef]
27. Wächter, A.; Biegler, L.T. On the implementation of an interior-point filter line-search algorithm for large-scale nonlinear programming. *Math. Program.* **2006**, *106*, 25–57. [CrossRef]
28. He, S.; Ding, F.; Lu, C.; Qi, Y. Impact of connected and autonomous vehicle dedicated lane on the freeway traffic efficiency. *Eur. Transp. Res. Rev.* **2022**, *14*, 1–14. [CrossRef]
29. Ghiasi, A.; Hussain, O.; Qian, Z.S.; Li, X. A mixed traffic capacity analysis and lane management model for connected automated vehicles: A Markov chain method. *Transp. Res. Part Methodol.* **2017**, *106*, 266–292. [CrossRef]
30. Martin-Gasulla, M.; Sukennik, P.; Lohmiller, J. Investigation of the impact on throughput of connected autonomous vehicles with headway based on the leading vehicle type. *Transp. Res. Rec.* **2019**, *2673*, 617–626. [CrossRef]
31. Varaiya, P. Max pressure control of a network of signalized intersections. *Transp. Res. Part Emerg. Technol.* **2013**, *36*, 177–195. [CrossRef]
32. Webster, F.V. *Traffic Signal Settings*; Technical report; Road Research Laboratory: London, UK, 1958.
33. Genders, W.; Razavi, S. An open-source framework for adaptive traffic signal control. *arXiv* **2019**, arXiv:1909.00395.
34. Gershenson, C. Self-organizing traffic lights. *arXiv* **2004**, arXiv:nlin/0411066.
35. Cools, S.B.; Gershenson, C.; D'Hooghe, B. Self-organizing traffic lights: A realistic simulation. In *Advances in Applied Self-Organizing Systems*; Springer: London, UK, 2013; pp. 45–55.
36. Lillicrap, T.P.; Hunt, J.J.; Pritzel, A.; Heess, N.; Erez, T.; Tassa, Y.; Silver, D.; Wierstra, D. Continuous control with deep reinforcement learning. *arXiv* **2015**, arXiv:1509.02971.
37. Casas, N. Deep deterministic policy gradient for urban traffic light control. *arXiv* **2017**, arXiv:1703.09035.